Phytomedicine 20 (2013) 394–400

Contents lists available at SciVerse ScienceDirect

Phytomedicine

journal homepage: www.elsevier.de/phymed

Lucidone from *Lindera erythrocarpa* Makino fruits suppresses adipogenesis in 3T3-L1 cells and attenuates obesity and consequent metabolic disorders in high-fat diet C57BL/6 mice

Yu-Hsin Hsieh[a,d], Sheng-Yang Wang[a,b,c,*]

[a] *Molecular and Biological Agricultural Sciences Program, Taiwan International Graduate Program, National Chung Hsing University and Academia Sinica, Taiwan*
[b] *Agricultural Biotechnology Research Center, Academia Sinica, Taipei, Taiwan*
[c] *Department of Forestry, National Chung-Hsing University, Taichung, Taiwan*
[d] *Graduate Institute of Biotechnology, National Chung Hsing University, Taichung, Taiwan*

ARTICLE INFO

Keywords:
Lucidone
Lindera erythrocarpa
Adipogenesis
High-fat diet
Obesity

ABSTRACT

Obesity is associated with an increased risk of development of numerous diseases including type 2 diabetes, hypertension, hyperlipidemia, and cardiovascular disease. In this study, we investigated the effects of lucidone *in vitro* on gene expression during adipogenesis in 3T3-L1 cells and *in vivo* on high-fat diet induced obesity in C57BL/6 mice. Lucidone at 40 μmol/L suppressed adipogenesis in 3T3-L1 cells by reducing transcription levels of adipogenic genes, including PPARγ, C/EBPα, LXR-α, LPL, aP2, GLUT4 and adiponectin. Five-week-old male C57BL/6 mice fed a high fat diet (60% energy from fat) supplemented with lucidone at a dosage of 1250 mg/kg of diet for 12 weeks had reduced body and liver weight, reduced epididymal and perirenal adipose tissue, decreased food efficiency (percentage of weight gain divided by food intake), and lowered plasma cholesterol, triglyceride, glucose, and insulin levels. Dissection of adipose tissue from lucidone-treated mice showed a reduction in the average fat-cell size and percentage of large adipocytes. These results provide evidence that dietary intake of lucidone alleviates high fat diet-induced obesity in C57BL/6 mice and reveals the potential of lucidone as a nutraceutical to prevent obesity and consequent metabolic disorders.

Introduction

Incidence of obesity worldwide has expanded dramatically over the last two decades due to diet and lifestyle changes. Obesity is associated with an increased risk for the development of numerous diseases including type 2 diabetes, hypertension, hyperlipidemia, and cardiovascular disease (Nawrocki and Scherer 2005). The development of obesity involves extensive adipose tissue remodeling by adipocyte hypertrophy, adipocyte hyperplasia and angiogenesis (Avram et al. 2007). Adipocyte hypertrophy results from an excessive accumulation of lipids from energy intake such as a high fat (HF) diet. Changes in adipocyte number result from a complex interplay between proliferation and differentiation of preadipocytes (Gregoire 2001).

Green and colleagues established the 3T3-L1 preadipocyte cell line, which has accelerated our knowledge of the mechanism of preadipocyte differentiation, or adipogenesis, at the molecular level (Green and Kehinde 1975). Several studies have demonstrated natural compounds with a potential to suppress adipogenesis in 3T3-L1 cells and, further, prevent obesity in animal models. For example, berberine inhibits adipocyte differentiation through the PPARγ pathway and reduces the expression of adipogenic enzymes (Choi et al. 2006; Huang et al. 2006). In addition, berberine reduces body weight gain and blood glucose in HF diet induced obesity mice (Xie et al. 2011) and decreased blood lipid level both in obese individuals and in SD rats (Hu et al. 2012). Curcumin suppresses preadipocyte differentiation and retards body weight gain in diet induced obesity (DIO) mice (Ejaz et al. 2009) *via* attenuating lipogenesis in the liver (Shao et al. 2012). Epigallocatechin gallate (EGCG) inhibits the adipocyte differentiation process *via* activating AMP-activated protein kinase (Hwang et al. 2005) and inhibiting the PPARγ pathway (Lin et al. 2005), further alleviating fatty liver disease in DIO mice (Bose et al. 2008). These studies

Abbreviations: PPARγ, peroxisome proliferator-activated receptor γ; C/EBP, CCAAT-enhancer-binding protein; LXR-α, liver X receptor α; LPL, lipoprotein lipase; aP2, adipocyte protein 2; GLUT4, glucose transporter type 4; ND, normal diet; HFD, high fat diet; LSH/L, lucidone-supplemented HFD at the lower dosage, 0.025%; LSH/H, lucidone-supplemented HFD at the higher dosage, 0.125%; DIO, diet-induced obesity.

* Corresponding author at: Department of Forestry, National Chung-Hsing University, 250 Kuo-Kuang Road, Taichung 402, Taiwan. Tel.: +886 4 22840345x138; fax: +886 4 22873628.
E-mail address: taiwanfir@dragon.nchu.edu.tw (S.-Y. Wang).

0944-7113/$ – see front matter © 2012 Elsevier GmbH. All rights reserved.
http://dx.doi.org/10.1016/j.phymed.2012.11.007

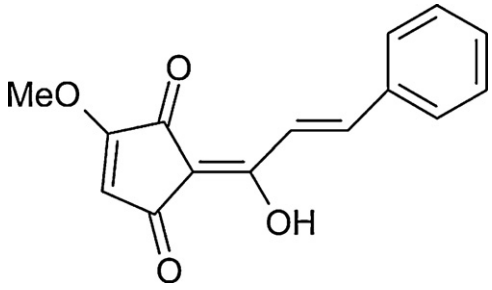

Fig. 1. Chemical structure of lucidone.

suggest that natural products that suppress adipogenesis in 3T3-L1 cells may have bioactivity *in vivo* that prevents body weight gain under unhealthy eating habits.

Lucidone (Fig. 1) is one of the major constituents of the fruit of *Lindera erythrocarpa* Makino (Wang et al. 2008). The fruit is used as a folk medicine for analgesic, digestive, diuretic, antidote and antibacterial purposes. Our previous studies have showed the anti-inflammatory effects of lucidone in RAW 264.7 cells (Kumar and Wang 2009) and ICR mice (Senthil Kumar et al. 2010). Hepatoportective effect against alcohol-induced oxidative stress in human hepatic cells (Senthil Kumar et al. 2012). The novel bioactivity of lucidone was investigated in this study; we determined the effects of lucidone on adipocyte differentiation process at the molecular level in 3T3-L1 cells, and the effects of dietary lucidone in high fat diet-fed C57BL/6 mice on body weight changes, physiological and metabolic variables and adipocyte size distribution.

Materials and methods

Phytocompound

Lucidone was prepared from *L. erythrocarpa* according to previously described protocols (Wang et al. 2008). The purity of the compound obtained was higher than 99.5% based on the results of HPLC and ^{1}H NMR analyzed.

Cell culture and stimulation

The 3T3-L1 cells were purchased from the Bioresource Collection and Research Center (Hsinchu, Taiwan). Cells were grown in Dulbecco's Modified Eagle's Medium (DMEM) supplemented with 10% bovine serum (BS), 100 units/ml penicillin and 100 μg/ml streptomycin (GIBCO, Invitrogen, Carlsbad, CA) at 37 °C in a 5% CO_2-humidified incubator. Cell differentiation was stimulated with a mixture of 1 μmol/l dexamethasone, 0.52 mmol/l isobutylmethylxanthine and 0.17 μmol/l insulin (Sigma–Aldrich) starting at 2 days postconfluence (designated as day 0) for 4 days (day 1 to day 4). The stimulation medium was then replaced with maintenance medium (DMEM supplemented with 10% FBS) for another 4 days (day 5 to day 8). To evaluate the effect of lucidone on adipogenesis, the indicated concentrations of lucidone were added at day 0 and day 4 when refreshing culture medium.

Oil Red O staining

The 3T3-L1 adipocytes were washed with PBS and then fixed with 4% paraformaldehyde for 1 h at room temperature. The supernatant was discarded and washed with deionized water. Cells were stained for 10 min at room temperature with freshly prepared 0.3% Oil Red O solution. To quantify the relative lipid content accumulated in cells, Oil Red O dye was eluted with 100% isopropanol and incubated for 10 min with gentle shaking and the absorbance at 510 nm was detected using an ELISA microplate reader (μQuant, Bio-Tek Instruments, Winooski, VT). The results were confirmed by three independent experiments.

Table 1
Sequences of primers used for qRT-PCR.

18S forward	5′-CGC CGC TAG AGG TGA AAT TCT-3′
18S reverse	5′-CAT TCT TGG CAA ATG CTT TCG-3′
PPARγ forward	5′-CAA GAA TAC CAA AGT GCG ATC AA-3′
PPARγ reverse	5′-GAG CTG GGT CTT TTC AGA ATA ATA AG-3′
C/EBPα forward	5′-AGC AAC GAG TAC CGG GTA CG-3′
C/EBPα reverse	5′-TGT TTG GCT TTA TCT CGG CTC-3′
LPL forward	5′-GGC CAG ATT CAT CAA CTG GAT-3′
LPL reverse	5′-GCT CCA AGG CTG TAC CCT AAG-3′
Adiponectin forward	5′-TCC TGG AGA GAA GGG AGA GAA AG-3′
Adiponectin reverse	5′-TCA GCT CCT GTC ATT CCA ACA T-3′
aP2 forward	5′-AGT GAA AAC TTC GAT GAT TAC ATG AA-3′
aP2 reverse	5′-GCC TGC CAC TTT CCT TGT G-3′
GLUT4 forward	5′-GAT TCT GCT GCC CTT CTG TC-3′
GLUT4 reverse	5′-ATT GGA CGC TCT CTC TCC AA-3′
LXR-α forward	5′-AGG AGT GTC GAC TTC GCA AA-3′
LXR-α reverse	5′-CTC TTC TTG CCG CTT CAG TTT-3′

Quantitative real-time PCR analysis

Cellular RNA was extracted from 3T3-L1 cells after MDI induction at different time points, 0.5 h, 1 day, 2 days, 4 days, 6 days and 8 days, using TRIzol reagent according to the manufacturer's instructions (Invitrogen). The complementary DNA was synthesized using high-capacity cDNA reverse transcription kits (Applied Biosystems, Carlsbad, CA) according to the manufacturer's instructions. Gene expression levels were analyzed using StepOne Real-Time PCR System (Applied Biosystems). The analyses for the genes including β-actin (Mm00607939_s1), C/EBPβ (Mm00843434_s1) and C/EBPδ (Mm00786711_s1) were conducted using Hot Start Fluorescent PCR ROX Core Kit (Tagman) (BIO Basic, Canada). The complementary DNA was denatured at 94 °C for 4 min, followed by 40 cycles of PCR (94 °C, 30 s; 60 °C, 30 s). The analyses for the genes described in Table 1 were conducted using Power SYBR Green PCR Master Mix (Applied Biosystems). The complementary DNA was denatured at 95 °C for 10 min, followed by 40 cycles of PCR (95 °C, 15 s; 60 °C, 60 s). β-Actin and 18S ribosomal RNA were used as the endogenous control independently in the comparative cycle-threshold method.

Animal maintenance and experimental setup

Three-week-old male C57BL/6 mice were obtained from Bio-LASCO (Taiwan). The mice were housed in groups of 4 per cage, under standard temperature-controlled conditions with a 12 h/12 h light-dark cycle and free access to food and water throughout the experiments. All animal experiments were conducted in accordance with the Guide for the Care and Use of Laboratory Animals and Taiwan laws relating to the protection of animals, and were approved by the local ethics committee. Before the experiments, mice were fed with certified rodent diet provided energy 14.4 kJ/g which is 24.1% from protein, 13.2% from fat and 62.7% from carbohydrates (5002, LabDiet, St. Louis, Missouri, USA) for 2 weeks. The micronutrient and macronutrient compositions were previously described (Keenan et al. 1997). At the beginning of the experiment, mice were randomly divided into 4 groups of 8 mice each. Three experimental groups were fed with a high-fat diet (HFD) (DIO rodent purified diet w/60% energy from fat, 58Y1, TestDiet) which provided 21.4 kJ/g of energy that was 18.1% from protein, 61.6% from fat and 20.3% from carbohydrates (Table 2) with or without dietary lucidone supplementation at two dosages, 250 mg/kg of diet (LSH/L, lucidone-supplemented HFD at the lower dosage, 0.025%) and 1250 mg/kg of diet (LSH/H, lucidone-supplemented HFD at the higher dosage, 0.125%). The control group was fed with certified

Table 2
Composition of normal diet and high fat diet.

	Normal diet	HF diet
Protein, %	20.7	23.1
Carbohydrate, %	53.8	25.9
Fiber, %	4.3	6.5
Fat, %	5.0	34.9
Cholesterol, *ppm*	140	301
Linoleic acid, %	2.2	4.7
Linolenic acid, %	0.2	0.4
Arachidonic acid, %	<0.01	0.06
Omega-3 fatty acids, %	0.4	0.4
Total saturated fatty acids, %	1.0	13.7
Total monounsaturated fatty acid, %	1.0	14.0
Energy, *kJ/g*	14.4	21.4
Protein, *% of energy*	24.1	18.1
Carbohydrate, *% of energy*	62.7	20.3
Fat, *% of energy*	13.2	61.6

rodent diet (ND). The total food intake by each cage of mice was recorded every 2 days, and the body weight of each mouse was recorded every 4 days. After dietary treatments for 12 weeks, the mice were feed-deprived for 16 h and killed by isoflurane (Halocarbon, NJ, USA). Blood, liver, kidney and adipose tissue were collected for further analysis.

Histological and morphometric analyses

Epididymal adipose tissue (EAT) and perirenal adipose tissue (PAT) were fixed in 4% buffered paraformaldehyde, dehydrated in a graded series of 70–100% ethanol, infiltrated in xylene and embedded in paraffin. Multiple sections of 3 μm were stained using standard procedures for hematoxylin and eosin staining. Images were acquired using a digital microscope (Olympus, Tokyo) and analyzed systematically with respect to adipocyte size and number using Image-Pro Plus software. The sizes of adipocytes were divided into 4 classes: 0–50 μm, 51–100 μm, 101–150 μm and 151–300 μm in diameter.

Biochemical analysis of plasma samples

Plasma concentration of creatinine, glucose, triglyceride, total cholesterol, HDL, and LDL were determined. All analyses were carried out in quadruplicate according to the spectrophotometry of Chiron Diagnostics Corporation (Oberlin, OH, USA) using the Express Plus Automatic Clinical Chemistry Analyzer (Chiron). Plasma concentrations of insulin were measured using commercial kits according to manufacturer's instructions (# EZRMI-13K, rat/mouse insulin 96-well plate assay, Millipore, MA, USA).

Statistical analysis

Data are expressed as means ± SEM. For *in vitro* studies, differences between the control and treated groups were evaluated by Student's *t*-test. For *in vivo* studies, one-way ANOVA was used to compare the differences among the ND, HFD, LSH/L and LSH/H groups. Tukey's test was used for multiple comparisons. For all analyses, $p < 0.05$ was considered statistically significant. All statistical analyses were performed using GraphPad Prism version 5.00 for Windows.

Results

In vitro studies

Lucidone suppresses adipocyte differentiation in a dose dependent manner

Two-day postconfluent 3T3-L1 cells were treated with lucidone at the indicated concentrations for 4 days in MDI induction medium and a further 4 days in maintenance medium. After adipogenesis, lucidone suppressed adipocyte differentiation by decreasing lipid droplet accumulation inside the cells (Fig. 2a). Oil Red O staining showed that the lipid content in lucidone-treated cells was reduced in a dose dependent manner compared with DMSO-treated control cells ($p = 0.74$, $p = 0.45$, $p < 0.01$, $p < 0.01$, $p < 0.001$, respectively) (Fig. 2b).

Effect of lucidone on differentiated adipocytes

After MDI induction for 8 days, mature adipocytes were treated with lucidone at a concentration of 40 μmol/l for a further 2–8 days (days 10–16 after MDI treatment). In comparison with the vehicle

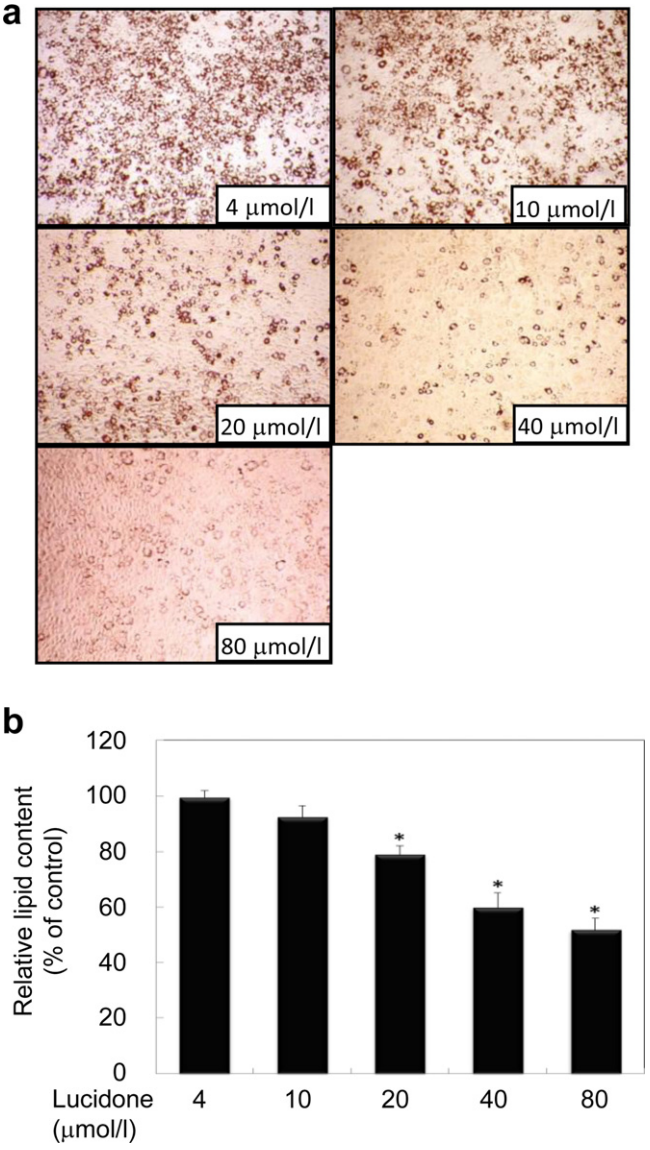

Fig. 2. Lucidone suppresses adipogenesis in a dose-dependent manner in 3T3-L1 cells as measured by Oil Red O stain (a) and quantified by ELISA reader (b). Values are expressed as the means ± SEM; $^*p < 0.01$ *vs.* control.

control, lucidone-treated cells showed no significant differences in either morphology or lipid content as quantified by Oil Red O staining at various time points (0 d, $p = 0.25$; 2 d, $p = 0.38$; 4 d, $p = 0.54$; 6 d, $p = 0.44$; 8 d, $p = 0.19$) (Supplemental Fig. 1).

Lucidone regulates transcription levels of adipogenic transcription factors and target genes

During cell differentiation, cells treated with lucidone showed a slightly higher level of C/EBPβ and C/EBPδ mRNA at the early stage compared with the control (Fig. 3a). In contrast, the mRNA levels of the adipogenic regulators PPARγ and C/EBPα were downregulated by lucidone treatment (Fig. 3b). We further tested genes that are highly transcribed in adipocytes such as liver X receptor α (*LXR-α*), lipoprotein lipase (*LPL*), adipocyte protein 2 (*ap2*), adiponectin and glucose transporter type 4 (*GLUT4*) (Fig. 3c). The transcription levels of these genes were dramatically reduced compared with the control, especially at the late stage of adipogenesis.

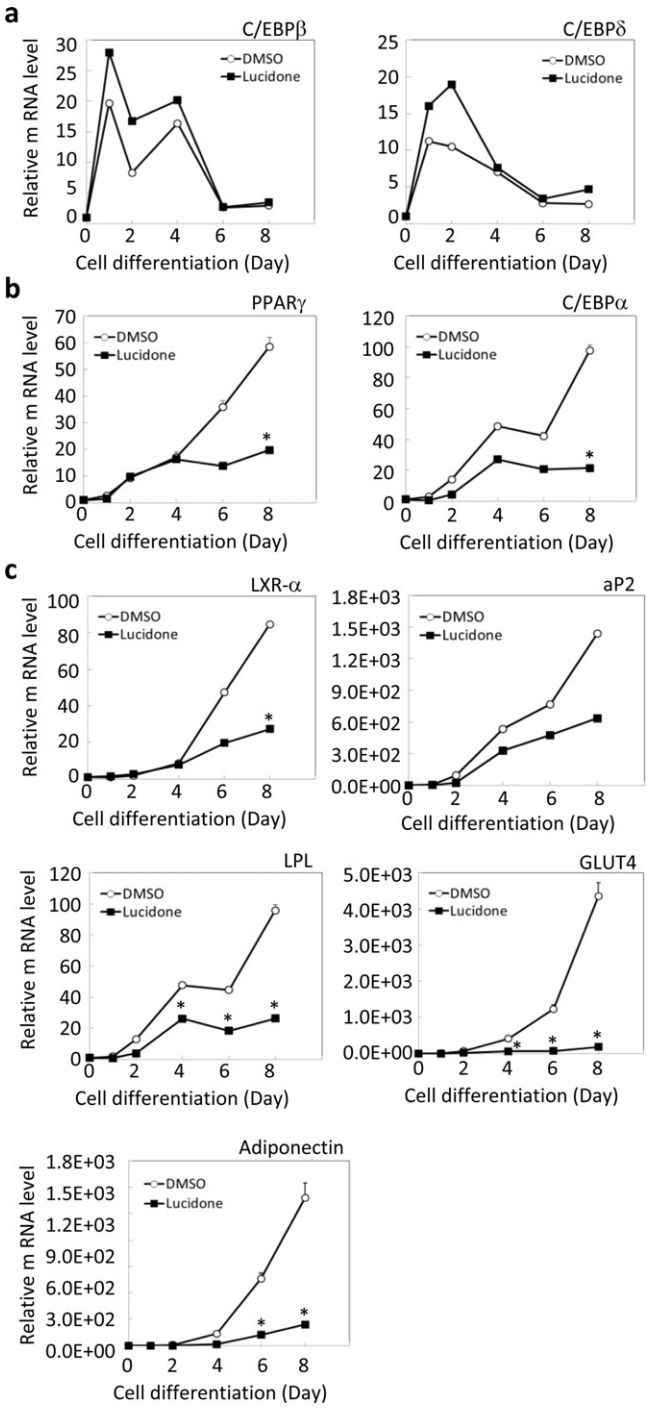

Fig. 3. Effects of lucidone on gene transcription patterns during adipogenesis, including C/EBPβ and C/EBPδ (a), PPARγ, C/EBPα (b) LXR-α, LPL, aP2, GLUT4 and adiponectin (c). The total RNA was isolated at different time points after MDI induction (0.5 h, 1 d, 2 d, 4 d, 6 d and 8 d). Values are expressed as the means ± SEM. Means at a time with a label differ; $^{*}p < 0.05$ *vs.* control.

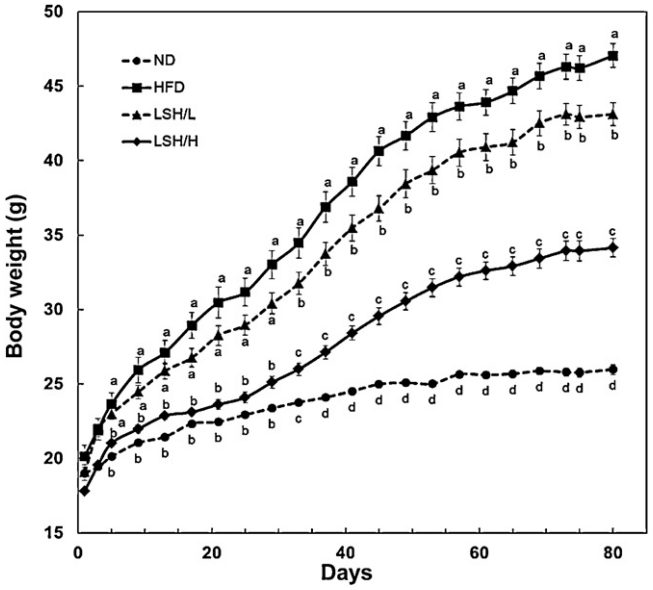

Fig. 4. Effects of dietary lucidone administered for 12 weeks on body weight changes. Values are expressed as the means ± SEM, $n = 8$. Means at a time point without a common letter differ; $p < 0.05$.

In vivo studies

Effect of dietary lucidone on physiological variables

The HF diet consistently increased body weight gain in C57BL/6 mice, but supplementing the HF diet with 0.125% lucidone dramatically suppressed the changes ($p < 0.0001$) (Fig. 4) without affecting body length ($p = 0.06$) (Table 3). LSH/L and LSH/H mice showed a lower daily food intake compared with HFD mice ($p < 0.001$). LSH/H mice showed a reduction in BMI value ($p < 0.001$) and food efficiency ($p = 0.05$) compared with HFD mice. HFD mice had enlarged livers (1.43 ± 0.09) ($p < 0.01$) compared with ND mice but liver size was normal in LSH/H mice (1.06 ± 0.04) ($p = 0.87$ compared with ND mice). Mice in all groups showed no change in kidney size ($p = 0.7$).

Effect of dietary lucidone on metabolic variables

There were no differences in blood creatinine concentration in any of the groups ($p = 0.1$) (Table 4). The fasting plasma glucose concentration was higher in HFD mice ($p < 0.001$) compared with ND mice but reduced in LSH/L ($p = 0.05$) and LSH/H ($p < 0.05$) mice. The fasting insulin level was higher in HFD mice ($p < 0.05$) compared with ND mice and was normalized in LSH/H mice ($p = 0.2$ compared with ND mice). Plasma concentration of TG, total cholesterol, HDL-C and LDL-C were higher in HFD mice but reduced in LSH/H mice ($p < 0.01$, $p < 0.001$, $p = 0.16$, $p < 0.05$, respectively).

Effect of dietary lucidone on fat pad mass and adipocyte size

HFD mice showed a higher total fat pad mass (EAT and PAT) ($p < 0.0001$) but fat pad mass was reduced in LSH/H mice ($p < 0.001$) (Table 5). Histological analysis of EAT and PAT showed that lucidone treatment affected the diameter (Fig. 5) and the distribution of cell-size in fat pads. The cell sizes of EAT and PAT in LSH/H mice

Table 3
Effects of dietary lucidone on physiological parameters in C57BL/6 mice fed a HF diet for 12 weeks.[a]

	ND	HFD	LSH/L	LSH/H
Body weight gain, *g*	7.0 ± 0.4[c]	26.9 ± 0.11[a]	24.1 ± 1.0[a]	16.7 ± 0.1[b]
Body length, *cm*	7.93 ± 0.17	9.17 ± 0.11[a]	9.1 ± 0.12[a]	8.76 ± 0.14[a]
BMI, g/cm^2	0.37 ± 0.01[c]	0.53 ± 0.02[a]	0.50 ± 0.01[a]	0.43 ± 0.02[b]
Daily food intake, *g*	3.13 ± 0.06[a]	2.68 ± 0.04[b]	2.53 ± 0.03[c]	2.22 ± 0.02[d]
Food efficiency, *%*	0.81 ± 0.03[c]	2.46 ± 0.07[a]	2.35 ± 0.39[a]	1.85 ± 0.12[b]
Liver weight, *g*	1.07 ± 0.03[b]	1.43 ± 0.09[a]	1.3 ± 0.08[a]	1.06 ± 0.04[b]
Kidney weight, *g*	0.31 ± 0.01	0.33 ± 0.02	0.34 ± 0.02	0.34 ± 0.02

[a] Values are means ± SEM, $n = 8$. Means in a row with superscripts letters without a common letter differ, $p < 0.05$. BMI: body mass index.

Table 4
Effects of dietary lucidone on metabolic variables in C57BL/6 mice fed a HF diet for 12 weeks.[a]

	ND	HFD	LSH/L	LSH/H
Creatinine, *μmol/l*	37.6 ± 2.21	37.6 ± 2.21	42.0 ± 2.21	33.2 ± 2.21
Glucose, *mmol/l*	6.8 ± 0.59[c]	18.1 ± 1.57[a]	13.0 ± 1.38[b]	11.6 ± 0.27[bc]
Insulin, *pmol/l*	47.0 ± 7.7[c]	205 ± 43.5[a]	103 ± 31.0[ab]	68.8 ± 12.5[bc]
TG, *mmol/l*	0.81 ± 0.07[c]	1.34 ± 0.03[a]	1.20 ± 0.09[ab]	1.01 ± 0.02[b]
Cholesterol, *mg/dl*	2.20 ± 0.18[c]	4.60 ± 0.14[a]	4.39 ± 0.23[ab]	3.72 ± 0.17[b]
HDL-C, *mmol/l*	1.28 ± 0.08[b]	3.06 ± 0.04[a]	2.93 ± 0.1[a]	2.17 ± 0.4[a]
LDL-C, *mmol/l*	0.16 ± 0.10[c]	0.43 ± 0.01[a]	0.33 ± 0.04[b]	0.32 ± 0.01[b]

[a] Values are means ± SEM, $n = 4$. Means in a row with superscripts letters without a common letter differ, $p < 0.05$.

Table 5
Effects of dietary lucidone on weight changes of adipose tissue and adipocyte size distribution in C57BL/6 mice fed a HF diet for 12 weeks.[a]

	ND	HFD	LSH/L	LSH/H
Total fat pad, *g*	0.57 ± 0.06[c]	3.88 ± 0.20[a]	3.7 ± 0.08[a]	2.74 ± 0.14[b]
EAT, *g*	0.41 ± 0.04[c]	2.72 ± 0.19[a]	2.6 ± 0.05[a]	1.91 ± 0.10[b]
Adipocyte diameter, *μm*	83.2 ± 2.8[c]	159.6 ± 12.1[a]	131.9 ± 8.4[ab]	120.1 ± 6.1[b]
Adipocyte diameter				
0–50 *μm, %*	42.9 ± 4.9[b]	3.4 ± 0.4[a]	5.1 ± 0.4[a]	8.5 ± 0.8[a]
51–100 *μm, %*	56.5 ± 2.8[b]	35.6 ± 1.0[a]	50.4 ± 1.5[b]	57.5 ± 1.4[b]
101–150 *μm, %*	0.6 ± 0.3[b]	33.3 ± 0.7[a]	29.9 ± 1.1[a]	27.6 ± 1.6[a]
151–300 *μm, %*	0 ± 0[c]	27.7 ± 0.4[a]	14.5 ± 0.4[b]	6.4 ± 0.3[c]
PAT, *g*	0.16 ± 0.03[c]	1.17 ± 0.06[a]	1.10 ± 0.07[a]	0.83 ± 0.05[b]
Adipocyte diameter, *μm*	85.2 ± 3.3[b]	135.0 ± 11.7[a]	128.3 ± 10.9[a]	117.9 ± 4.9[a]
Adipocyte diameter				
0–50 *μm, %*	31.4 ± 9.0[b]	4.7 ± 0.5[a]	5.8 ± 0.8[a]	12.4 ± 1.4[a]
51–100 *μm, %*	66.3 ± 6.3[b]	56.4 ± 1.9[b]	56.8 ± 2.5[b]	68.4 ± 2.9[a]
101–150 *μm, %*	2.4 ± 1.7[c]	24.2 ± 1.2[b]	33.7 ± 1.0[a]	15.1 ± 1.2[c]
151–300 *μm, %*	0 ± 0[b]	14.8 ± 0.5[a]	3.7 ± 0.7[b]	4.2 ± 0.7[b]

[a] Values are means ± SEM, $n = 6$–8. For cell counting, $n > 100$. Means in a row with superscripts letters without a common letter differ, $p < 0.05$.

were reduced compared with HFD mice ($p < 0.001$). In EAT, the percentage of adipocytes with diameters of 101–150 and 151–300 μm was greater in HFD mice and gradually reduced in LSH/L ($p = 0.3$, $p < 0.01$) and LSH/H ($p = 0.06$, $p < 0.0001$) mice. The proportion of adipocytes with diameters of 0–50 and 51–100 μm was lower in HFD mice and gradually increased in LSH/L ($p = 0.4$, $p < 0.05$) and LSH/H ($p = 0.03$, $p < 0.0001$) mice. The cell size distribution in PAT of LSH/H mice showed a similar tendency, with a higher proportion

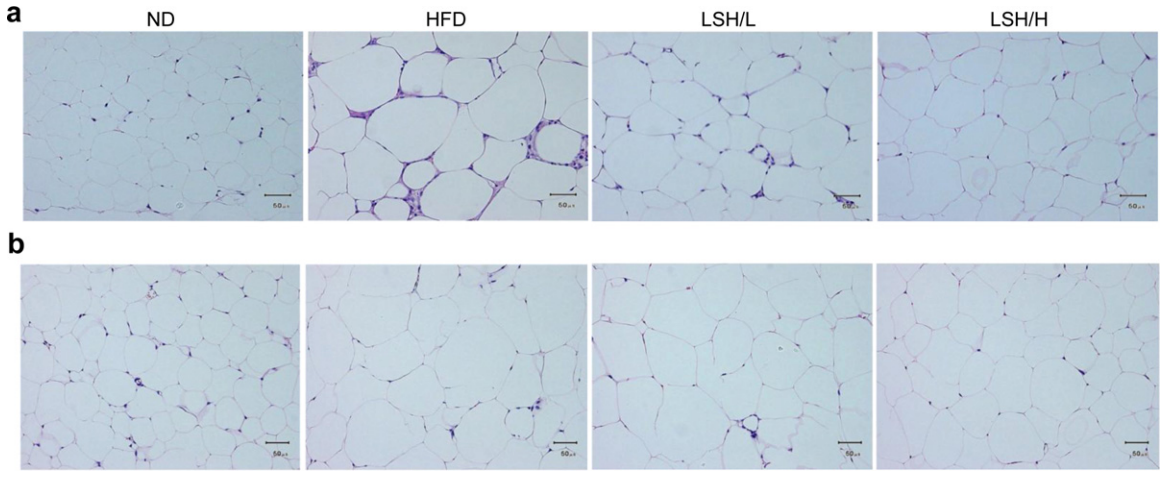

Fig. 5. Histology of EAT (a) and PAT (b) by hematoxylin and eosin stain from ND, HFD, LSH/L and LSH/H mice; $n = 6$.

of 0–50 ($p = 0.1$) and 51–100 μm ($p < 0.01$) and lower percentage of 101–150 ($p = 0.1$) and 151–300 μm ($p < 0.01$) diameter cells compared with HFD mice.

Discussion

In this study, we evaluated the effects of lucidone on adipocyte differentiation in mouse 3T3-L1 cells and showed that lucidone remarkably reduced lipid content in a dose dependent manner. As the reduction of lipid accumulation in cells during adipogenesis may have resulted from a decrease in lipogenesis and/or an increase in lipolysis, mature adipocytes were treated with or without lucidone for a further 2–8 days. As these mature lucidone-treated adipocytes showed no further changes compared with control, we suggest that lucidone treatment reduced lipid accumulation in 3T3-L1 cells by suppressing adipogenesis rather than promoting lipolysis.

At the molecular level, C/EBPβ and C/EBPδ rapidly respond to adipogenic induction and trigger 3T3-L1 differentiation (Cao et al. 1991). In the middle stage of adipogenesis, the master regulators of adipogenesis PPARγ and C/EBPα, synergistically induce the transcription of downstream genes to transform preadipocytes into mature adipocytes (Ntambi and Young-Cheul 2000). Our data showed that during adipogenesis lucidone-treated 3T3-L1 preadipocytes had slightly increased mRNA levels of C/EBPβ and C/EBPδ in the early stage but showed remarkable suppression of PPARγ and C/EBPα transcription. These results indicate that lucidone suppresses adipogenesis through downregulating PPARγ and C/EBPα and the effect is independent of the initiator, C/EBPβ and C/EBPδ. LXR-α, a regulator for a transcription of fatty acid synthase, was suppressed by lucidone after 4 days of cell differentiation. We also demonstrated that lucidone treatment lowered the transcription level of several genes that are highly expressed in mature adipocytes such as LPL, aP2, adiponectin and GLUT4. Lucidone thus showed comprehensive suppression of adipogenesis at the molecular level.

Acute toxicity studies of the ethyl acetate fraction of the fruit in ICR mice in series dosages up to 2 g/kg B.W. showed no toxicity according to measurements of both physiological and metabolic variables. In this study, we found that dietary lucidone (0.125%, LSH/H) for 12 weeks remarkably reduced body weight gain in mice fed a HF diet and the effect persisted over time. Although LSH/H mice consumed less energy per day, the value of food efficiency (percentage of weight gain divided by food intake) decreased gradually in lucidone-treated groups revealing that loss of body weight was not only caused by energy intake. Dietary lucidone may encourage a higher basal metabolism or a higher body temperature. Dietary lucidone (0.125%) diminished the mass of both EAT and PAT by approximately 30% (Table 5). This may be a result of the reduction of the average diameter of adipocytes and rearrangement in cell-size distribution in the fat pad. Histological analysis showed that cells of over 151 μm in diameter efficiently decreased in fat pads from LSH/L mice. This effect may be due to suppression of adipogenic genes by lucidone and concomitant inhibition of adipocyte differentiation and hypertrophy.

PPARγ deficiency leads to lipodystrophy. Common clinical features of lipodystrophic patients are insulin resistance, dyslipidemia and hypertension (Tontonoz and Spiegelman 2008). Adipose-specific knockout mice showed insulin resistance in fat and liver, hepatomegaly, fat cell loss and compensatory hypertrophy. Adipose-specific PPARγ knockout mice fed with a HF diet for 5 weeks showed a diminution of body weight gain and adipose size but an enhancement of plasma insulin concentration compared with control mice (He et al. 2003). The higher plasma insulin was suggested to be because of insulin resistance. In our study, lucidone treatment reduced not only adipose size, but also plasma insulin and glucose concentration. The enlarged liver caused by HF diet was normalized by dietary lucidone. The beneficial effects of lucidone on improving hyperinsulinemia and hepatomegaly were not consistent with the phenomena in PPARγ knockout mice. Moreover, heterozygous PPARγ-deficient mice decreased lipogenesis in the liver, increased β-oxidation and mitochondrial uncoupling protein 2 in the liver and muscle (Yamauchi et al. 2001). Taken together, we propose that lucidone not abolished PPARγ transcription but attenuated the excess PPARγ transcription caused by fat-rich food, thus suppressing lipogenesis and promoting energy dissipation to alleviate obesity and related lesion.

Dyslipidemia is caused by unhealthy food and/or lifestyles, such as diets rich in carbohydrate, fat and cholesterol or being overweight. Moreover, elevated levels of cholesterol and LDL-C are associated with an increased risk of coronary heart disease (CHD) (Wilson et al. 1998). Although the LDL/HDL-C ratio, a risk factor for CHD, was not significantly decreased by lucidone treatment in this study, HFD mice showed an increasing level of plasma cholesterol, HDL-C, LDL-C and TG, which were gradually reduced in LSH/L and LSH/H mice (Table 4). The decrease TG content may result from decreasing lipid synthesis and further increased in insulin sensitivity in LSH/H mice.

In conclusion, our study demonstrated that lucidone suppressed 3T3-L1 adipocyte differentiation by downregulating the transcription of master regulators of adipogenesis PPARγ and C/EBPα. Furthermore, lucidone repressed the transcription level of genes involved in lipogenesis including *LXR-α*, *LPL*, *aP2*, *adiponectin* and *GLUT4*. Dietary intake of lucidone in mice fed with a HF diet reduced body weight gain, epididymal and perirenal fat accumulation presumably resulting from a reduction in adipocyte diameter. Mice fed a HF diet with lucidone improved hyperglycemia, hyperinsulinemia, dyslipidemia and hepatomegaly without kidney lesion. Our study clearly shows that consumption of lucidone as a nutraceutical can aid prevention of obesity and consequent metabolic disorders. The mechanism of action of lucidone in obesity prevention needs further investigation.

Conflict of interest

The authors declared no conflict of interest.

Acknowledgments

This work was supported by Council of Agriculture (100AS-8.4.1-FB-e1) and the Molecular and Biological Agricultural Sciences Program, Taiwan International Graduate Program, National Chung Hsing University and Academia Sinica.

Appendix A. Supplementary data

Supplementary data associated with this article can be found, in the online version, at http://dx.doi.org/10.1016/j.phymed.2012.11.007.

References

Avram, M.M., Avram, A.S., James, W.D., 2007. Subcutaneous fat in normal and diseased states 3. Adipogenesis: from stem cell to fat cell. Journal of the American Academy of Dermatology 56, 472–492.

Bose, M., Lambert, J.D., Ju, J., Reuhl, K.R., Shapses, S.A., Yang, C.S., 2008. The major green tea polyphenol, (−)-epigallocatechin-3-gallate, inhibits obesity, metabolic syndrome, and fatty liver disease in high-fat-fed mice. The Journal of Nutrition 138, 1677–1683.

Cao, Z., Umek, R.M., McKnight, S.L., 1991. Regulated expression of three C/EBP isoforms during adipose conversion of 3T3-L1 cells. Genes and Development 5, 1538–1552.

Choi, B.H., Ahn, I.S., Kim, Y.H., Park, J.W., Lee, S.Y., Hyun, C.K., Do, M.S., 2006. Berberine reduces the expression of adipogenic enzymes and inflammatory molecules of 3T3-L1 adipocyte. Experimental and Molecular Medicine 38, 599–605.

Ejaz, A., Wu, D., Kwan, P., Meydani, M., 2009. Curcumin inhibits adipogenesis in 3T3-L1 adipocytes and angiogenesis and obesity in C57/BL mice. The Journal of Nutrition 139, 919–925.

Green, H., Kehinde, O., 1975. An established preadipose cell line and its differentiation in culture II. Factors affecting the adipose conversion. Cell 5, 19–27.

Gregoire, F.M., 2001. Adipocyte differentiation: from fibroblast to endocrine cell. Experimental Biology and Medicine 226, 997–1002.

He, W., Barak, Y., Hevener, A., Olson, P., Liao, D., Le, J., Nelson, M., Ong, E., Olefsky, J.M., Evans, R.M., 2003. Adipose-specific peroxisome proliferator-activated receptor gamma knockout causes insulin resistance in fat and liver but not in muscle. Proceedings of the National Academy of Sciences of the United States of America 100, 15712–15717.

Hu, Y., Ehli, E.A., Kittelsrud, J., Ronan, P.J., Munger, K., Downey, T., Bohlen, K., Callahan, L., Munson, V., Jahnke, M., Marshall, L.L., Nelson, K., Huizenga, P., Hansen, R., Soundy, T.J., Davies, G.E., 2012. Lipid-lowering effect of berberine in human subjects and rats. Phytomedicine 19, 861–867.

Huang, C., Zhang, Y., Gong, Z., Sheng, X., Li, Z., Zhang, W., Qin, Y., 2006. Berberine inhibits 3T3-L1 adipocyte differentiation through the PPARgamma pathway. Biochemical and Biophysical Research Communications 348, 571–578.

Hwang, J.T., Park, I.J., Shin, J.I., Lee, Y.K., Lee, S.K., Baik, H.W., Ha, J., Park, O.J., 2005. Genistein, EGCG, and capsaicin inhibit adipocyte differentiation process via activating AMP-activated protein kinase. Biochemical and Biophysical Research Communications 338, 694–699.

Keenan, K.P., Ballam, G.C., Dixit, R., Soper, K.A., Laroque, P., Mattson, B.A., Adams, S.P., Coleman, J.B., 1997. The effects of diet, overfeeding and moderate dietary restriction on Sprague–Dawley rat survival, disease and toxicology. The Journal of Nutrition 127, 851S–856S.

Kumar, K.J., Wang, S.Y., 2009. Lucidone inhibits iNOS and COX-2 expression in LPS-induced RAW 264.7 murine macrophage cells via NF-kappaB and MAPKs signaling pathways. Planta Medica 75, 494–500.

Lin, J., Della-Fera, M.A., Baile, C.A., 2005. Green tea polyphenol epigallocatechin gallate inhibits adipogenesis and induces apoptosis in 3T3-L1 adipocytes. Obesity Research 13, 982–990.

Nawrocki, A.R., Scherer, P.E., 2005. Keynote review: the adipocyte as a drug discovery target. Drug Discovery Today 10, 1219–1230.

Ntambi, J.M., Young-Cheul, K., 2000. Adipocyte differentiation and gene expression. The Journal of Nutrition 130, 3122S–3126S.

Senthil Kumar, K.J., Hsieh, H.W., Wang, S.Y., 2010. Anti-inflammatory effect of lucidone in mice via inhibition of NF-kappaB/MAP kinase pathway. International Immunopharmacology 10, 385–392.

Senthil Kumar, K.J., Liao, J.W., Xiao, J.H., Gokila Vani, M., Wang, S.Y., 2012. Hepatoprotective effect of lucidone against alcohol-induced oxidative stress in human hepatic HepG2 cells through the up-regulation of HO-1/Nrf-2 antioxidant genes. Toxicology In Vitro 26, 700–708.

Shao, W., Yu, Z., Chiang, Y., Yang, Y., Chai, T., Foltz, W., Lu, H., Fantus, I.G., Jin, T., 2012. Curcumin prevents high fat diet induced insulin resistance and obesity via attenuating lipogenesis in liver and inflammatory pathway in adipocytes. PLoS ONE 7, e28784.

Tontonoz, P., Spiegelman, B.M., 2008. Fat and beyond: the diverse biology of PPARgamma. Annual Review of Biochemistry 77, 289–312.

Wang, S.Y., Lan, X.Y., Xiao, J.H., Yang, J.C., Kao, Y.T., Chang, S.T., 2008. Antiinflammatory activity of *Lindera erythrocarpa* fruits. Phytotherapy Research: PTR 22, 213–216.

Wilson, P.W., D'Agostino, R.B., Levy, D., Belanger, A.M., Silbershatz, H., Kannel, W.B., 1998. Prediction of coronary heart disease using risk factor categories. Circulation 97, 1837–1847.

Xie, W., Gu, D., Li, J., Cui, K., Zhang, Y., 2011. Effects and action mechanisms of berberine and Rhizoma coptidis on gut microbes and obesity in high-fat diet-fed C57BL/6J mice. PLoS ONE 6, e24520.

Yamauchi, T., Kamon, J., Waki, H., Murakami, K., Motojima, K., Komeda, K., Ide, T., Kubota, N., Terauchi, Y., Tobe, K., Miki, H., Tsuchida, A., Akanuma, Y., Nagai, R., Kimura, S., Kadowaki, T., 2001. The mechanisms by which both heterozygous peroxisome proliferator-activated receptor gamma (PPARgamma) deficiency and PPARgamma agonist improve insulin resistance. The Journal of Biological Chemistry 276, 41245–41254.